



## Science Arts & Métiers (SAM)

is an open access repository that collects the work of Arts et Métiers Institute of Technology researchers and makes it freely available over the web where possible.

This is an author-deposited version published in: <https://sam.ensam.eu>  
Handle ID: <http://hdl.handle.net/10985/22902>



This document is available under CC BY-NC-SA license

### To cite this version :

Gabriel MARGALIDA, Olivier ROUSSETTE, Jérôme DELVA, Antoine DAZIN, Pierric JOSEPH - Pulsed air injection system characterization for stall margin improvement in an axial compressor - In: 9TH EUROPEAN CONFERENCE FOR AERONAUTICS AND SPACE SCIENCES (EUCASS), France, 2022-06-27 - 9TH EUROPEAN CONFERENCE FOR AERONAUTICS AND SPACE SCIENCES (EUCASS) - 2022

Any correspondence concerning this service should be sent to the repository

Administrator : [scienceouverte@ensam.eu](mailto:scienceouverte@ensam.eu)



# Pulsed air injection system characterization for stall margin improvement in an axial compressor

*Gabriel Margalida\*, Pierric Joseph\*, Antoine Dazin\*, Olivier Roussette\*, Jérôme Delva\**

*\*Univ. Lille, CNRS, ONERA, Arts et Métiers Institute of Technology, Centrale Lille, UMR 9014 - LMFL - Laboratoire de Mécanique des Fluides de Lille - Kampé de Fériet*

*F-59000 Lille, France*

## Abstract

This paper presents the design and the characterization of a pulsed air injection system on a single stage axial compressor. The goal of this system is to delay the rotating stall onset and to extend the compressor operating range. The proposed control system consists in 20 injection blocks of 2 injectors, allowing to adjust some of the fluidic and geometrical parameters of the injected perturbations. Velocity, flow rate and momentum can be varied on a large range and the injectors can be rotated by 15° steps or replaced to change the yaw angle and the outlet section.

## Nomenclature

|                  |  |
|------------------|--|
| SM               | Surge margin                                   |
| SMI              | Stall margin improvement                       |
| $c$              | Rotor tip chord                                |
| $q$              | Single actuator mass flow rate                 |
| $f$              | Actuation frequency                            |
| $\alpha$         | Actuation duty cycle                           |
| $p$              | Actuators supply pressure                      |
| $\Delta P_{t-s}$ | Total to static pressure increase of the stage |
| $q_c$            | Mass flow rate of the main compressor flow     |
| $\Pi$            | Pressure ratio of the stage                    |

## 1. Introduction

Since the very beginning of gas turbines development, rotating stall and compressor surge have been an important limit in the operating range of the engines [1]. Many paper, event recent ones [2,3] have discussed the origin of rotating stall which is strongly linked with the flow dynamic in the tip region of the blade. This undesirable behavior happens when the operating point is brought toward the high - pressure ratio / low mass flow rate part of the performance curve. To prevent potentially dramatic events, significative security margins are applied to keep the operating point of the compressor far from the unstable area. This limits the maximum pressure ratio of each compressor stage and leads to the use of more stages, with, as a result, bulkier and heavier engines.

For decades now, a lot of research efforts have been put in Stall Margin Improvement (SMI). Casing treatments are a widely applied methods in this purpose [4], but these passive methods present the main drawback to permanently modify the flow inside the compressor, and then, to potentially have detrimental effects on the nominal operating point. Active control methods, which can be turned on and off as needed, have here a strong advantage.

Research work about range extension through active flow control was started several years ago with, for example, the study of Ludwig et al. [5]. A lot of research teams have then investigated such solutions, through various control technics. Continuous air injection is a popular choice thank to the availability of pressurized air in the downstream section of the compressor. Among all the available literature, one can cite the work of Suder et al. on an isolated stage [6] and Stöbel et al. on a real aircraft engine [7]. This kind of continuous flow control is certainly efficient for tip critical geometry as it strongly decreases the blade loading at tip, and thus delay the arising of the phenomena which are leading to stall [4]. Periodic blowing, on the other hand, was only seldom considered (see for example the study of Kefalakis et Papailiou [8]). This kind of forcing is known, in flow separation control for example, to present strong advantages compared to continuous blowing, like stronger effect with smaller energy consumption (see the extensive review of Greenblatt and Wagnanski [9]). When considering the pulsed jets actuation in particular, specific features

like fast adjustment of the mass flow rate through duty cycle variation [10] or overshoot at valves opening [11] could be of great interest for axial compressor applications.

Present paper details the design and characterization of a control system based on such principles, as a preliminary step to carry an experimental study of active control of rotating stall. A precise characterization of the performance of the injection system, usually summarily described in other reported works, will be given with a special attention to the performance in pulsed actuation which seems to be a promising way to adjust the injected flow rate. The test rig considered to implement this system is the CME2 compressor rig installed in the Lille Laboratory of Fluid Mechanics (Arts et Métiers Lille). This test installation is a single stage, low speed, axial compressor whose main parameters are summarized in Table 1.

Table 1: Compressor parameters

| Parameter   | Value | Unit |
|---|-------|------|
| Rotational speed                                  | 3200  | rpm  |
| Design mass flow rate at 3200rpm                  | 5.3   | kg/s |
| Design total to static pressure ratio at 3200 rpm | 1.03  |      |
| Rotor blade number                                | 30    |      |
| Stator blade number                               | 40    |      |
| Casing diameter                                   | 550   | mm   |
| Hub-tip ratio, leading edge                       | 0.75  |      |
| Hub-tip ratio, trailing edge                      | 0.78  |      |
| Rotor tip chord                                   | 84    | mm   |
| Rotor tip stagger angle                           | 54    | °    |
| Rotor tip gap                                     | 0.5   | mm   |
| Tip Mach Number at 3200 rpm                       | 0.28  |      |

More details about this rig are also available in previous papers [12,13]. CME2 compressor is considered as a semi - industrial test rig, as it exhibits smaller pressure ratio compare with the ones achieved in real machines. However, as demonstrated in the previous references, it reproduces quite well the flow physics associated with the rotating stall phenomena, with a tip leakage vortex clearly visible on the pressure maps measured at the casing.

The first part of this paper consists in a presentation of the design of the injection system itself. Key parameters identified from the literature are exposed, along with the technical constraints of the compressor environment.

The second part of the paper presents some experimental results of performance tests of an isolated actuator. These tests were realized on a dedicated test bench using mainly hot - wire anemometry at ambient room conditions. First subsection consists in a jet characterization with actuator operated in continuous mode. Performance in pulsed mode, with an emphasis on the temporal response of the actuator, is presented in the second subsection. The last subsection presents a quantitative assessment of the whole control system installed on the compressor as it will be used for further experiments of rotating stall control.

## 2. Design of the injection system

Previous works on the CME2 compressor [12] highlighted the “Tip Critical” nature of this geometry. It was consequently chosen to perform blowing at the casing, right into the tip gap. The strategy is here to add high momentum flow in the tip gap region to keep the flow attached as long as possible, delaying then the occurrence of rotating stall.

As demonstrated by Nie et al. [14], blowing performance increases as the distance from the blade decreases. In the present case, blowing is realized 10 mm (equal to  $0.12 \cdot c$ ) upstream to the rotor (see Figure 1a, closer location could have led to some unwanted alterations of the tip leakage flow with the modification of the casing). Nie et al. [14] also studied the effect of the yaw angle on a limited extend, along with Kefalakis & Papaillou [8]. As it could be interesting to push further these experiments, the possibility to adjust the yaw angle was retained in this design, through the rotation of the injectors. On the opposite, the pitch angle was set constant to  $0^\circ$  (parallel to the casing), to act only on the tip region of the blade. To do so, the injectors were designed (see also Figure 1a) to benefit from the Coandă effect and were manufactured using 3D printing.

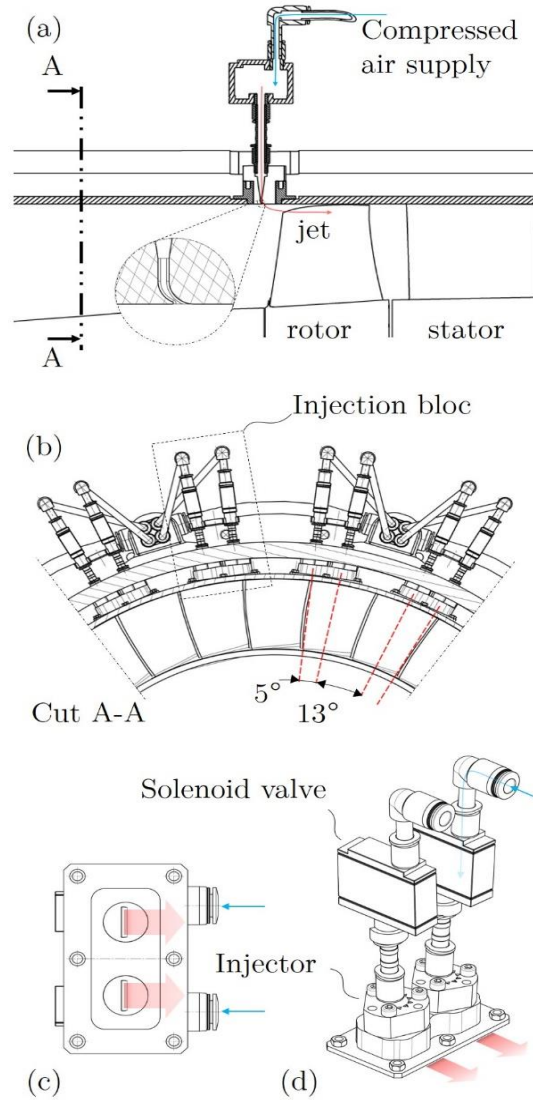


Figure 1: Some views of the control system: (a) injectors location in front of the rotor, (b) injectors distribution around the casing, (c) view of the exhaust ports from the inside of the compressor and (d) two injectors with associated magnetic valves

There is no real consensus in the literature concerning the number and angular arrangement of the injectors. For example, the study of Suder [6], which doesn't report any influence of the arrangement, appears to be in contradiction with some other works of Graf et al. [15] or Cumpsty et al. [16]. Nevertheless, Cassina et al [17] have clearly shown that a good angular cover was beneficial in terms of SMI improvement. Consequently, it has been chosen to extend as much as possible the width of the slots. Besides, too large slots are not compatible with the possibility of rotating the injectors. Indeed: size and geometrical form of the jet were also highly constrained by the environment. To avoid any protrusion of the injector in the main flow, the diameter of the injectors must be limited. Slot jets were preferred to achieve a good angular coverage (considering the finite number of injectors), and then the slot width was limited to 10 mm (see Figure 1c) but associated by pairs.

Finally, it has been chosen to use the arrangement described on Figure 1b (20 blocks of 2 injectors, as to say 40 injection points), as it constitutes a good trade - off between technical feasibility, angular coverage, and modularity of the system. It must be noted that each injector is equipped with an electromagnetic valve and that these valves are controlled independently of each other (see Figure 1d).

To achieve a time varying actuation, the control system relies on fast magnetic valves (Matrix MX 821, see Figure 1d), allowing up to 500 Hz commutation frequency under 8 bar supply pressure. These valves are feed by a pressurized tank instrumented with pressure and temperature sensors to measure the generating conditions. Flow rate is measured by two different flowmeters:

- Festo SFAM, up to 10 000 l/min, with a  $\pm (0.3\% \text{ FSO} + 3\% \text{ measured value})$  uncertainty.

- Festo SFAH, up to 200 l/min, with a  $\pm (1\% \text{ FSO} + 2\% \text{ measured value})$  uncertainty.

The first one is used to monitor the entire injection system performance, while the second is used to characterize an isolated injector.

Command signals of the valves were generated using an analog output electronic card (National Instruments PXIe - 6738), with an in - house code generating a periodic square signal with variable duty cycle. One recalls here a difference with more classical control systems applied on axial compressors in the literature, as this square signal is used to vary the injected mass flow, instead of, as more commonly done, the actuators supply pressure.

### 3. Characterization of the injection system

Flow velocity at the jet exhaust is investigated on a dedicated test bench located at the ONERA Lille center and the analysis relies on hot - wire anemometry. Single component straight probe (Dantec 55P11) is used to characterize the flow. Its positioning with respect to the jet exhaust is realized with the help of cameras, and the probe is mounted on a traverse system allowing displacements with an uncertainty less than 0.02 mm. The sensing element of the probe is a platinum plated wire, 5  $\mu\text{m}$  in diameter and 1.25 mm long, driven by a Dantec anemometer (MiniCTA). Calibration is performed prior each series of measurements and data are fitted within the range 1 m/s to 300 m/s. Sampling frequency is set to 20 kHz, and the number of samples is  $4 \times 10^4$ . Uncertainty on the measured velocity is estimated to less than  $\pm 1\%$  with a 95% confident interval for flow measurements, according to manufacturer data. In the following results, as single component probe is used, only the magnitude of the velocity is presented.

#### 3.1 Continuous mode

The actuator is first operated with the magnetic valve fully open and with a supply pressure ranging from  $p = 1$  to 8 bar (maximum working pressure of the valves). Velocity is first measured in a longitudinal (x,z) plane, then in a traversal (z,y) plane at  $x = 10$  mm downstream of the jet exhaust (see Figure 2). In both cases, measurements are performed with a  $\Delta z = 0.2$  mm and  $\Delta x = \Delta y = 0.5$  mm discretization. As indicated in Figure 2, area in the immediate vicinity of the wall were not mapped to avoid contact between the sensor and the wall. Consequently,  $z = 0$  corresponds to 0.3 mm from the wall.

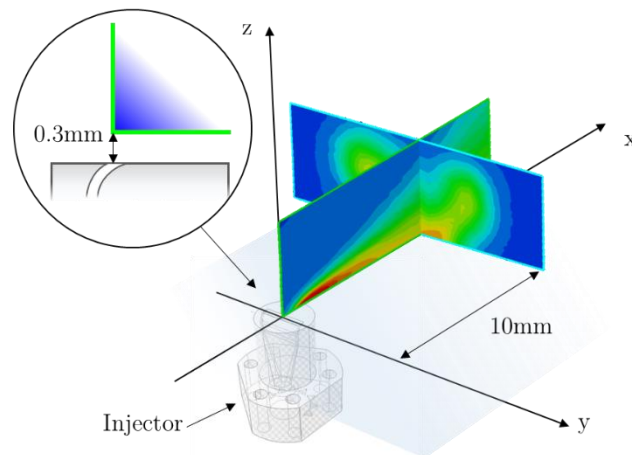


Figure 2: Location of the investigated area with respect to the jet exhaust

Figure 3 presents first results obtained in the longitudinal plane for a flow rate of  $q = 2$  g/s. Velocity up to 160 m/s are measured, and the jet appears confined very close to the wall, as velocity decays rapidly above  $z = 1$  mm. The Coandă

effect works here perfectly as the jet is nearly bended by 90° at the exit of the injector. Regarding the experiments on the compressor test rig, this means that the jets will stay close to the casing, and that its influence will be mainly concentrated on the tip gap area.

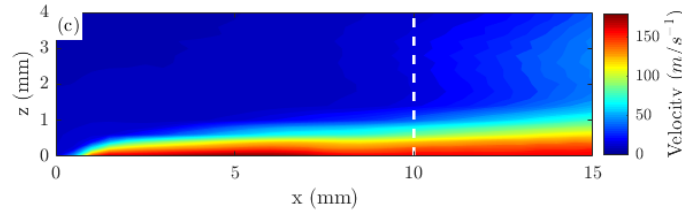


Figure 3: Map of velocity magnitude measured in the longitudinal (x,z) plan (continuous actuation,  $q = 2 \text{ g/s}$ )

Additional experiments are performed with different flow rates. A similar behavior is observed for most of the tested configurations, but for the smallest flow rates, vectorization of the jet appears to be far less established. Figure 4 presents some velocity profiles extracted at  $x = 10 \text{ mm}$  downstream in the symmetry plan ( $y = 0$ ) of the jets, for 3 different flow rates representative of the encountered situations. For  $q = 0.4 \text{ g/s}$ , one observes that significant velocity levels are still measured up to  $z = 2 \text{ mm}$ , which indicates that the injector shape struggles here to maintain the jet close to the wall. As such low flow rate configuration leads to small jet velocity, this behavior has been considered as acceptable, being not of primary interest for future stall control experiments.

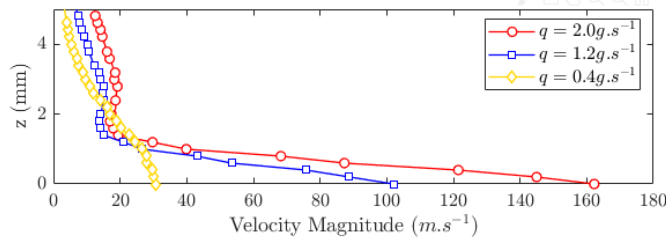


Figure 4: Mean profiles of velocity magnitude at  $x = 10 \text{ mm}$  downstream of the jet in the longitudinal ( $y = 0$ ) plan (continuous actuation)

Some investigations are also realized in the transversal direction ( $x = 10 \text{ mm}$  downstream of the jet exhaust), as presented in Figure 5. Recalling that exit section of the injector is a  $10 \text{ mm}$  slot, one observes that the jet width (estimated to a little bit less than  $8 \text{ mm}$ ) doesn't exactly match the injector geometry. It appears that some unexpected separations probably occur in the divergent section of the actuator, leading to an angular coverage smaller than expected. As this effect remains limited, it was chosen to keep this geometry for the first control experiments on the compressor, especially considering the very satisfactory behavior of the vectorization effect previously presented. One can also notice, on Figure 5, the particular shape of the flow on the edge of the jet, in the transversal direction. These flow structures are certainly associated with two axial vortices, generated by the strong shear flow existing at the edge of the jet.

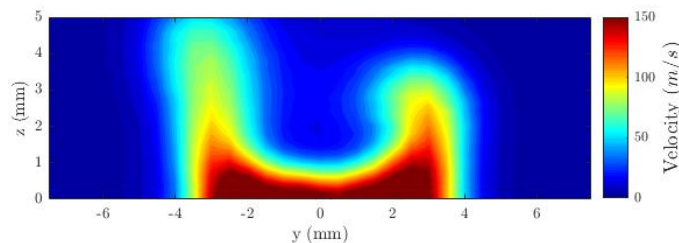


Figure 5: Map of velocity magnitude measured in the transversal (y,z) plan at  $x = 10 \text{ mm}$  (continuous actuation,  $q = 2 \text{ g/s}$ )

### 3.2 Pulsed actuation

Dynamic characterization of the time varying actuation in pulsed mode is realized thank to synchronous acquisition of the command signal of the actuator. Each actuation cycle is then identified and used to perform phase - locked averaging, as presented in Figure 6. The set of results corresponds to a supply pressure of  $p = 1.8$  bar with a duty cycle  $\alpha = 0.4$ , the probe being located at  $x = 2$  mm downstream of the jet exhaust, as close as possible to the wall ( $z = 0$  mm) and in the symmetry plane of the injector ( $y = 0$  mm). First results gathered at low frequencies (Figure 6a and Figure 6b) show that time series of jet velocity match the command signal and exhibit a square shape with a return to zero at the valve closing. The simultaneous recording of the command signal highlights a delay between this signal and the velocity time series, due to the time response of the valve estimated to 1 ms according to the manufacturer datasheet. This delay explains the degradation of the actuator behavior for higher frequency actuations (see for example  $f = 300$  Hz in Figure 6c), as the time response of the valve becomes comparable to the blowing time, as depicted by the marker at 1 ms, resulting of the “saw tooth” shaped signal depicted in Figure 6c. This limit will have to be considered for future control experiments.

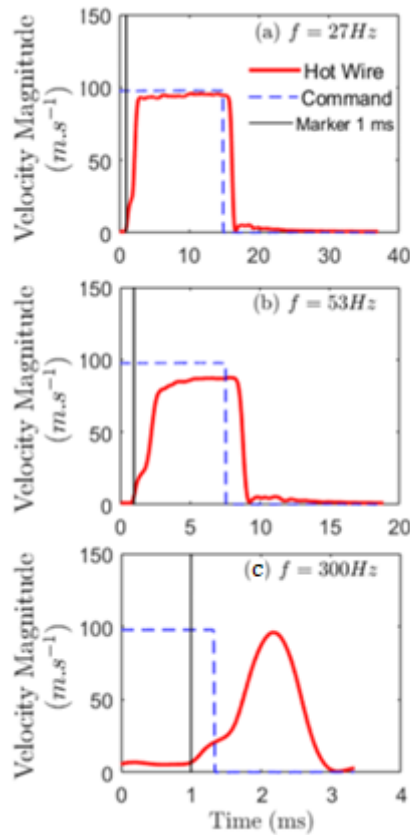


Figure 6: Phase - averaged time series of jet velocity magnitude for pulsed actuation at various frequencies ( $f = 27$  Hz, 53 Hz and 300 Hz,  $p = 1.8$  bar,  $\alpha = 0.4$  and measured at  $x = 2$  mm,  $y = z = 0$  mm)

Figures 6a and 6b also depict an unexpected behavior, as there are not any overshoot features as normally expected with this kind of setup (see also some previous work of the authors [18], in complement of the references given in the introduction). Deeper investigations are presented in Figure 7 to shed some light on this lack of velocity peak at the valve opening. In this figure, 2D phase - locked velocity maps are built using the command signal as phase reference. This case has been realized with the following parameters,  $\alpha = 0.4$ ,  $f = 100$  Hz and a supply pressure of  $p = 2.5$  bar. The four selected time steps correspond to the very beginning of the blowing phase, which normally presents the transient velocity peak characteristic of the overshoot phenomenon. By looking at the Figure 7b, one observes a very different behavior of the jet, if one compares it with Figure 7d where the pulsed jet is identical to the continuous one. In Figure 7b, the jet vectorization appears to be not fully established, and the jet leaves the injector with a nearly  $45^\circ$  angle, before reattaching to the wall a few milliseconds later.

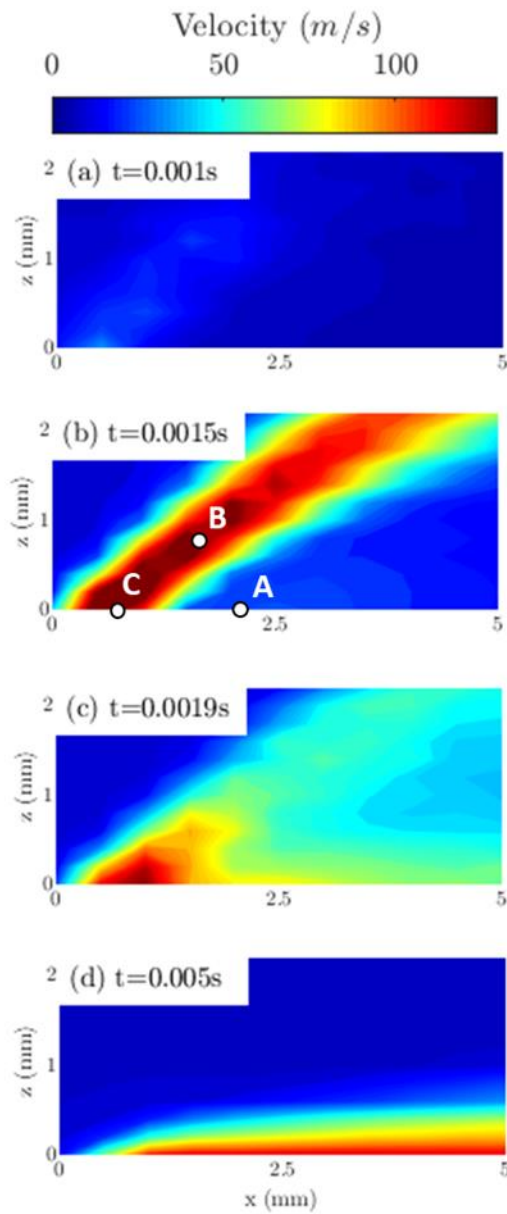


Figure 7: Mean phase - locked maps of velocity magnitude measured in the longitudinal (x,z) plan extracted at different time steps ( $f = 100$  Hz,  $p = 2.5$  bar,  $\alpha = 0.4$ )

This behavior is unexpected, but on the other side, it explains why the overshoot is not captured on the results presented on Figure 6, as the probe is positioned outside the initially detached jet (corresponding to position A on Figure 7b). To confirm this observation, times series of jet velocity are extracted at three different locations labeled as A, B and C on Figure 7b, and corresponding results are presented in Figure 8. Velocity overshoot at the valve opening is here clearly visible when the measurement is realized in an appropriate location (B and C).

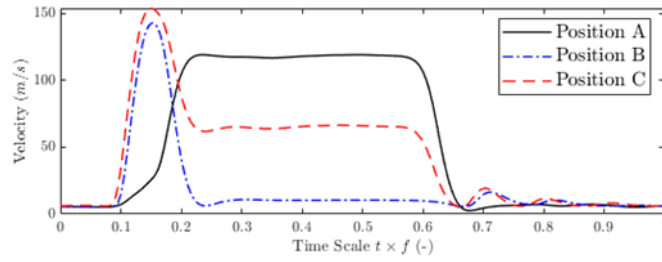


Figure 8: Phase - averaged time series of jet velocity magnitude for pulsed actuation ( $f = 100$  Hz,  $p = 2.5$  bar,  $\alpha = 0.4$ ) and measured at three different locations as marked on Figure 7

In the framework of the experiments on the compressor, this means that during the very beginning of the blowing phase, air is pulsed far from the tip gap for a short period of times. Thereby, the potential benefits of the high momentum flow carried by this overshoot could be thus “wasted”, from a control point of view. This does not question the whole design of the system (once again, especially considering its very good vectorization of the jet), but it is planned to elucidate and possibly to correct this unexpected behavior thanks to CFD analysis in a near future to propose an optimized version of these injectors. Consequently, additional experiments (results to be published) are being carried out, not in quiescent air, but in presence of an external flow (in wind tunnel, so with conditions closer to compressor applications). Preliminary observations seem to indicate that the transient phase is different in this case, and that the jet remains close to the wall during its establishment phase.

As one plans to use the duty cycle to vary the injected mass flow on the compressor, measurements have also been carried out with different  $\alpha$  values. These results are presented in Figure 9 and show how the mean flow rate can be dynamically adjusted by changing the duration of the blowing on each actuation cycle, without changing the supply pressure.

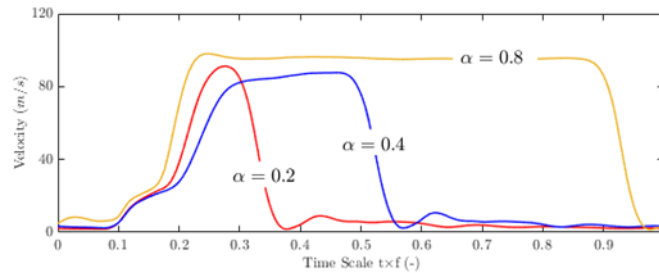


Figure 9: Phase - averaged time series of jet velocity magnitude for pulsed actuation ( $f = 100$  Hz,  $p = 1.9$  bar) for various duty cycle values and measured at  $x = 2$  mm,  $y = z = 0$  mm

Obviously, this method has some limitations, as for very small or very high  $\alpha$  values, the time response of the valve (opening and, respectively, closing time) becomes comparable to the blowing duration (leading to some cut off of the jet and so lower velocity levels). However, as depicted in Figure 9, this phenomenon doesn’t occur for  $0.2 < \alpha < 0.8$ , which let a sufficiently large parametric space to perform extensive experiments on the compressor test rig.

### 3.3 Complete system performance

Characterization of the control system is concluded by a validation of the whole system behavior once installed on the compressor rig, with the complete apparatus, including the additional compressor producing the supply pressure, various intermediary buffer tanks and the final tubing system. A first set of experiments is carried out to detect any dissimilarities between the forty injectors on the compressor. Results are presented in Figure 10 for two different levels of supply pressure. For both, all injectors appear to produce similar flow rates, as maximum measured difference is around 1%, laying down below the precision of the flowmeter as indicated by the error bars.

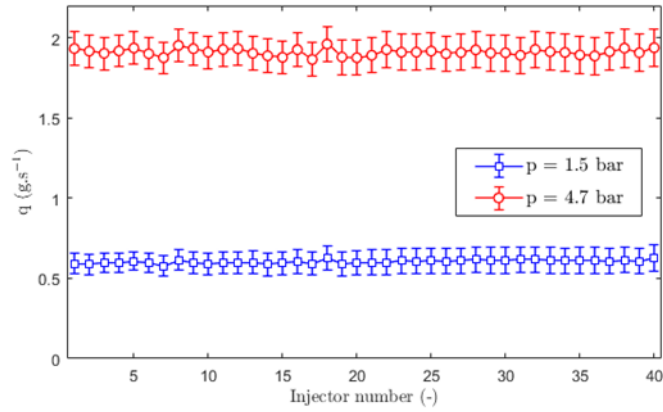


Figure 10: Mean flow rate measured in each injector once installed on the compressor test rig for two different levels of supply pressure with continuous actuation, error bars are measurement errors of the flowmeter

As one plans to use duty cycle variation to set the injected flow rate for a given level of supply pressure and actuation frequency, performance maps of the system have been realized, as for example the one presented on Figure 11 (color map gives the total flow rate for a set of duty cycle / supply pressure at a given value of actuation frequency). Thanks to this database, one can get a perfect knowledge of the injected mass flow in the compressor, and then quickly identify the best control configurations where high SMI are obtained with a minimal amount of injected mass flow. As a side note, maximum injected mass flow, with respect to the compressor mass flow rate, can be set up to 2.5% with continuous actuation and maximum supply pressure. This value was targeted, based on a literature review, to have a significant effect on the compressor performance with a limited injected energy.

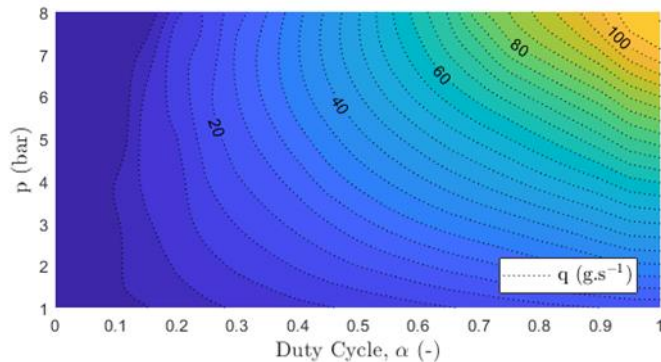


Figure 11: Sample of performance maps of the control system indicating the injected flow rate for various values of duty cycle and supply pressure for a given frequency ( $f = 100$  Hz for this map)

To conclude this section, Figure 12 presents a preliminary result of SMI obtained with this control system on the CME2 compressor. Performance curves are given without control and then with pulsed actuation ( $f = 100$  Hz and supply pressure  $p = 7.5$  bar) for five values of the duty cycle. One can observe that by varying  $\alpha$  from 0.2 to 1, the last stable point can be push proportionally further toward the low mass flow rate regions compared to the stability limit without control, but also with much higher - pressure ratio for every controlled cases.

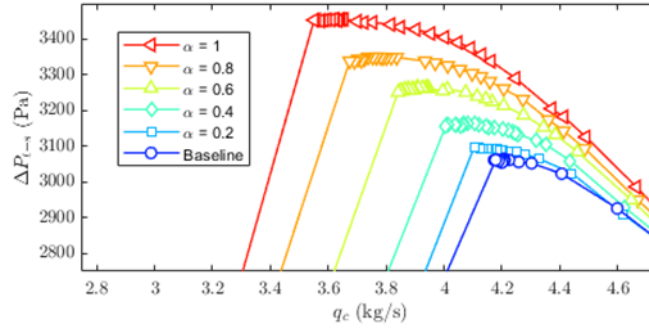


Figure 12: Stability improvements achieved on the compressor performance map by using the pulsed jets control system with various duty cycle values ( $p = 7.5$  bar,  $f = 100$  Hz and 20 injectors activated)

Using the definition from Weigl et al. [19] given by equations (1) and (2) (see Figure 13), these results lead to a SMI that can be freely adjusted from 10 % to 85% only through an update of the duty cycle. The injected mass flow rate varies from 0.32% to 1.6% of the compressor flow rate on this range. Please note that in equations (1) and (2) along with Figure 13, the subscripts “N” and “S” refer to quantities at the nominal operating point and, respectively, at the last stable operating point before stall (i.e., the operating point with the lowest flow rate before the stall onset). Similarly, subscript “B” refers to the baseline case without control, and “C” to the controlled case.

$$SM = \left( \frac{q_{c,N}}{q_{c,S}} \times \frac{\Pi_S}{\Pi_N} - 1 \right) \times 100 \quad (1)$$

$$SMI = \frac{SM_C - SM_B}{SM_B} \times 100 \quad (2)$$

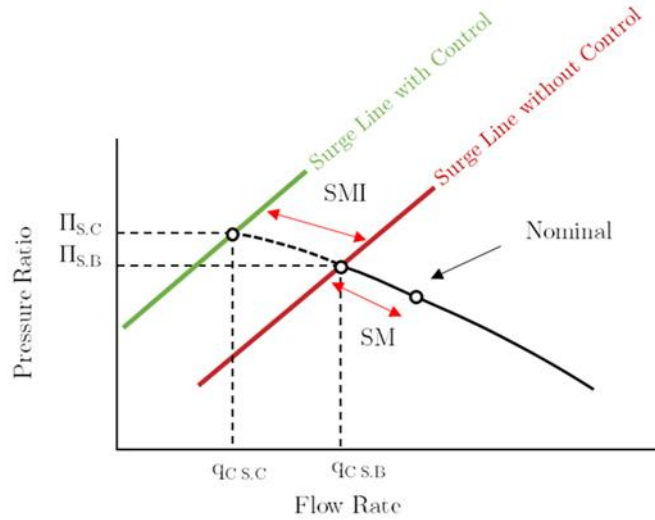


Figure 13: Schematic description of the SMI as defined by Weigl et al. [19]

## 4. CONCLUSION

Characterization of a control system designed for stability improvement of an axial compressor is presented in this paper. The first part has discussed some technical details and design choices, like the actuator type or injector location. When possible, these choices have been underpinned thanks to the literature. On a second part, a detailed analysis of the flow produced by an isolated actuator, without crossflow, is proposed, mainly based on hot - wire anemometry measurements. First results gathered in continuous mode reveals that the injector shape, based on Coandă effect, perfectly plays its role as the jet stays attached to the casing allowing a direct vectorization into the tip gap, except for the lowest investigated flow rate. Slight improvements could be made on the injector shape to overcome the limited

span wise extent of the jet, probably due to early separation in the diverging section. Characterization in pulsed mode reveals the expected overshoot at the valve opening, typical of pulsed actuation. However, this overshoot is detached from the casing, shooting at an angle of  $45^\circ$  relative to the axial direction, far from the tip gap. This effect is observed only during the very first instant of the blowing phase, and so do not question the whole design of the injector but let some place for improvements to properly exploit this high momentum flow for SMI. In addition, recent additional experiments may show that this effect is less pronounced in presence of an external flow. This subsection also demonstrates that the duty cycle is nicely suited to modify the injected mass flow of the control system, by varying the effective injection time on a blowing cycle. Last subsection presents a couple of results validating the whole control once installed on the compressor, showing that all the forty injectors behave similarly. This control system has been fully characterized and installed on the compressor rig. Next step is now to study its ability to postpone the occurrence of the rotating stall and to achieve significant SMI with a small energy cost. Preliminary results which are shown are promising, as SMI up to 90 % can be easily achieved.

The influence of several other parameters must be characterized to cope with some inconsistencies in the literature. Different yaw angles must be tested, along with different angular arrangement. A lot of attention will be given to the efficiency of the different tested configurations. One has good hope to greatly reduce the needed injected mass flow thank the time varying ability of the control system described in this paper. This research work will be associated in a near future to other activities carried out on this test rig on stall detection and describe in [11]. Thank to this coupled approach, one plans then to contribute to allow such control system to “pay its place” in an aircraft engine in the future.

## Acknowledgments

The present work was supported by the ANR project NUMERICCS (ANR-15-CE06-0009), and this project has received funding from the Clean Sky 2 Joint Undertaking under the European Union’s Horizon 2020 research and innovation programme under grant agreement No. 886352.

## References

- [1] I. J. Day, “Stall, Surge, and 75 Years of Research,” *J. Turbomach.*, vol. 138, no. 1, p. 011001, 2015, doi: 10.1115/1.4031473.
- [2] G. Pullan, A. M. Young, I. J. Day, E. M. Greitzer, and Z. S. Spakovszky, “Origins and Structure of Spike-Type Rotating Stall,” *J. Turbomach.*, vol. 137, no. 5, May 2015, doi: 10.1115/1.4028494.
- [3] M. Hewkin-Smith, G. Pullan, S. D. Grimshaw, E. M. Greitzer, and Z. S. Spakovszky, “The Role of Tip Leakage Flow in Spike-Type Rotating Stall Inception,” *J. Turbomach.*, vol. 141, no. 6, Jun. 2019, doi: 10.1115/1.4042250.
- [4] M. D. Hathaway, “Passive Endwall Treatments for Enhancing Stability,” NASA Rep. No. TM-2007-214409, no. July 2007, 2007.
- [5] G. R. Ludwig and J. P. Nenni, “A Rotating Stall Control System for Turbojet Engines,” *J. Eng. Power*, vol. 101, no. 3, pp. 305–313, Jul. 1979, doi: 10.1115/1.3446574.
- [6] K. L. Suder, M. D. Hathaway, S. A. Thorp, A. J. Strazisar, and M. B. Bright, “Compressor Stability Enhancement Using Discrete Tip Injection,” *J. Turbomach.*, vol. 123, no. 1, pp. 14–23, Jan. 2001, doi: 10.1115/1.1330272.
- [7] M. Stöbel, S. Bindl, and R. Niehuis, “Ejector Tip Injection for Active Compressor Stabilization,” in *Volume 2A: Turbomachinery*, 2014, vol. 2A, doi: 10.1115/GT2014-25073.
- [8] M. Kefalakis and K. D. Papailiou, “Active Flow Control for Increasing the Surge Margin of an Axial Flow Compressor,” in *Volume 6: Turbomachinery, Parts A and B*, 2006, vol. 2006, no. 4241X, pp. 101–111, doi: 10.1115/GT2006-90113.
- [9] D. Greenblatt and I. Wygnanski, “The control of flow separation by periodic excitation,” *Prog. Aerosp. Sci.*, vol. 36, no. 7, pp. 487–545, Oct. 2000, doi: 10.1016/S0376-0421(00)00008-7.
- [10] T. Shaqarin, C. Braud, S. Coudert, and M. Stanislas, “Open and closed-loop experiments to identify the separated flow dynamics of a thick turbulent boundary layer,” *Exp. Fluids*, vol. 54, pp. 1448–1470, 2013.
- [11] J. Ortmanns, M. Bitter, and C. J. Kähler, “Dynamic vortex structures for flow-control applications,” *Exp. Fluids*, vol. 44, no. 3, pp. 397–408, Jan. 2008, doi: 10.1007/s00348-007-0442-8.
- [12] M. Vegliò, A. Dazin, G. Bois, and O. Roussette, “Unsteady pressure measurements of spike type inception in axial compressor: Time frequency analysis and averaging procedure,” in *11th European Conference on Turbomachinery Fluid Dynamics and Thermodynamics, ETC 2015*, 2015.
- [13] G. Margalida, A. Dazin, P. Joseph, and O. Roussette, “Detailed Pressure Measurements During the Transition to Rotating Stall in an Axial Compressor: Influence of the Throttling Process,” in *Volume 1: Flow Manipulation and Active Control; Bio-Inspired Fluid Mechanics; Boundary Layer and High-Speed Flows; Fluids Engineering Education; Transport Phenomena in Energy Conversion and Mixing; Turbulent Flows; Vortex Dynamics; DNS/LES and Hybrid RANS*, 2018, p. V001T01A001, doi: 10.1115/FEDSM2018-83057.

- [14] C. Nie, G. Xu, X. Cheng, and J. Chen, "Micro Air Injection and Its Unsteady Response in a Low-Speed Axial Compressor," *ASME Conf. Proc.*, vol. 2002, no. 3610X, pp. 343–352, 2002, doi: 10.1115/GT2002-30361.
- [15] M. B. Graf et al., "Effects of Non-Axisymmetric Tip Clearance on Axial Compressor Performance and Stability," in *Volume 1: Aircraft Engine; Marine; Turbomachinery; Microturbines and Small Turbomachinery*, 1997, doi: 10.1115/97-GT-406.
- [16] N. A. Cumpsty, "Part-Circumference Casing Treatment and the Effect on Compressor Stall," in *Volume 1: Turbomachinery*, 1989, doi: 10.1115/89-GT-312.
- [17] G. Cassina, B. H. Beheshti, A. Kammerer, and R. S. Abhari, "Parametric Study of Tip Injection in an Axial Flow Compressor Stage," in *Volume 6: Turbo Expo 2007, Parts A and B*, 2007, pp. 137–145, doi: 10.1115/GT2007-27403.
- [18] P. Joseph, X. Amandolèse, and J.-L. Aider, "Drag reduction on the 25° slant angle Ahmed reference body using pulsed jets," *Exp. Fluids*, vol. 52, no. 5, pp. 1169–1185, Dec. 2012, doi: 10.1007/s00348-011-1245-5.
- [19] H. J. Weigl et al., "Active Stabilization of Rotating Stall and Surge in a Transonic Single Stage Axial Compressor," in *Volume 4: Manufacturing Materials and Metallurgy; Ceramics; Structures and Dynamics; Controls, Diagnostics and Instrumentation; Education; IGTI Scholar Award*, 1997, doi: 10.1115/97-GT-411.